Switchable and Functional Fluorophores for Multidimensional Single-Molecule Localization Microscopy

Yunshu Liu[1], Md Abul Shahid,[1] Hongjing Mao,[1] Jiahui Chen,[1] Michael Waddington,[1] Ki-Hee Song,[2,*] and Yang Zhang[1,*]

[1]Molecular Analytics and Photonics (MAP) Laboratory, Department of Textile Engineering, Chemistry and Science, North Carolina State University, Raleigh, NC 27606, USA

[2]Quantum Optics Research Division, Korea Atomic Energy Research Institute, Yuseong-gu, Daejeon 34057, Republic of Korea

ABSTRACT: Multidimensional Single-Molecule Localization Microscopy (mSMLM) represents a paradigm shift in the realm of super-resolution microscopy techniques. It affords the simultaneous detection of single-molecule spatial locations at the nanoscale and the functional information by interrogating the emission properties of switchable fluorophores. The latter are finely tuned to report their local environment through carefully manipulated laser illumination and single-molecule detection strategies. This Perspective highlights recent strides in mSMLM with a focus on fluorophore designs and their integration with mSMLM imaging systems. Particular interests are the accomplishments in simultaneous multiplexed super-resolution imaging, nanoscale polarity and hydrophobicity mapping, and single-molecule orientational imaging. Challenges and prospects in mSMLM are also discussed which include the development of more vibrant and functional fluorescent probes, the optimization of optical implementation to judiciously utilize the photon budget, and the advancement of imaging analysis and machine learning techniques.

KEYWORDS: Switchable Fluorophores; Fluorescent Probes; Super-Resolution Microscopy; SMLM; Spectroscopic Imaging; Polarity Mapping; Orientational Imaging; Fluorescence Lifetime Imaging

Introduction

Single-Molecule Localization Microscopy (SMLM) techniques such as Photoactivated Localization Microscopy (PALM) and Stochastic Optical Reconstruction Microscopy (STORM) are a collection of acclaimed super-resolution optical imaging techniques that enable the visualization of nanoscale architectures and molecular interactions in three dimensions (3D) with an exceptional spatial resolution down to 10 nm.[1–5] SMLM captures the fluorescence intermittency (often referred to as stochastic single-molecule "blinking") of individual switchable fluorescent probes that are labeled to the (bio)molecules of interest and reconstruct a super-resolution map with 3D coordinates of every emitting molecule.[1] Beyond capturing spatiotemporal information (x, y, z, time) of individual molecules using single-molecule tracking[6], recent advances in SMLM have allowed us to decode the polarity-[7–11], diffusivity-[12–14], and orientational information[15–17] of the fluorescent probes by capturing the fluorescence spectra[18–24], polarization[16,25,26], lifetime[27,28], etc. The imaging of these additional dimensions in SMLM has offered unprecedented opportunities to investigate nanoscopic functional information, which is referred to as multidimensional SMLM or mSMLM[29].

In order to perform mSMLM, it is crucial to identify fluorescent probes that convey distinct features besides stochastic fluorescence switching[30], depending on the specific dimension of interest. For instance, the detection of single-molecule polarization is benefitted from the use of fluorescent probes with a relatively large dipole moment to facilitate the discrimination of two orthogonal polarized emission signals.[16] Similarly, the super-resolution polarity mapping exploits the polarity-sensitive fluorescent dyes[10,31] and detects their single-molecule fluorescence spectral features in polar versus non-polar local environments. To advance mSMLM towards a better understanding of structurally, dynamically, and functionally intricate biological systems, the development of functional and switchable fluorophores that convey the signals in a particular dimension is indispensable.

In recent years, substantial progress has been made in the design and synthesis of switchable fluorescent probes with improved photophysical properties, high brightness, and high photostability for SMLM, as extensively reviewed in the literature.[30,32–35] In this Perspective, we specifically focus on the developments of (1) simultaneously photoswitchable fluorophore sets, (2) polarity-sensitive and switchable fluorescent sensors, (3) orientation-sensitive fluorescent

probes, and (4) fluorophores enabling fast super-resolution diffusivity measurements. We also discussed their integration with various mSMLM imaging techniques including spectroscopic SMLM (sSMLM)[36], spectroscopic Point Accumulation In Nanoscale Topography (sPAINT)[8] single-molecule orientation localization microscopy (SMOLM)[16], single-molecule diffusivity mapping (SM*d*M)[13], fluorescence-lifetime SMLM (FL-SMLM).[27] Furthermore, we will provide insights into current challenges and future directions in fluorescent probe design, optical implementation, and imaging analysis to advance our understanding of biological processes using mSMLM.

Simultaneous photoswitchable fluorophore sets for parallel, multiplexed mSMLM

A simultaneous photoswitchable fluorophore set is referred to as a set of fluorophores that can photoswitch/activate their fluorescence under very similar illumination and buffer conditions. Typically, the set of fluorophores should share similar absorption peaks (λ_{abs}) that allow simultaneous excitation using a single laser line. In addition, the set of fluorophores needs to possess statistically resolvable single-molecule emission signatures such as single-molecule emission peaks (λ_{smEm}) or fluorescence lifetime (τ_f) for single-molecule discrimination and multi-color mSMLM imaging. Each dye species in the simultaneous switchable fluorophore sets needs to be orthogonally labeled to the different imaging targets (*e.g.,* different proteins, lipids, DNA) using immunofluorescence staining, stable or transient genetic expression of self-labeling tags, or specific ligands to co-label the biomolecules with minimal cross-reactivity similar to the dye labeling requirement for multiplexed SMLM.[3,37]

However, unlike conventional multi-color PALM/STORM-based SMLM imaging[1] which requires the set of photoswitchable fluorophores (*e.g.,* Cy3 and Cy5) to have fully resolved emission spectra (*e.g.,* emission peaks of 568 nm and 670 nm), in mSMLM the set of fluorophores only needs to have distinct single-molecule emission signatures (*e.g.,* λ_{smEm} of 670 nm and 680 nm) regardless of their emission spectral overlaps. These statistically distinguishable single-molecule emission features minimize single-molecule misidentifications[38] caused by imaging background noise and single-molecule fluorescence heterogeneity thus enabling multiplexed mSMLM imaging. We discussed the three major sets of simultaneous photoswitchable synthetic fluorophores for sSMLM and FL-SMLM imaging as well as simultaneous photoswitchable fluorescent proteins used in sSMLM below.

Synthetic photoswitchable fluorophore sets for multiplexed sSMLM

More than a dozen synthetic photoswitchable fluorophores commonly used for SMLM[18,23,39,40] have been investigated for their use as sets of fluorophores for simultaneous multiplexed sSMLM imaging. Most reported multiplexed sSMLM sets use cyanine-based far-red photoswitchable fluorophores including Dyomics 634 (Dy634), Alexa Fluor 647 (AF647), Dylight 650, CF660C, Cy5.5, and CF680 (representative dye structures are shown in **Fig. 1A**). These probes can be all excited using a single far-red laser line with wavelengths around 640-647 nm at a power density of 2-20 kW cm^{-2} in an oxygen-scavenging

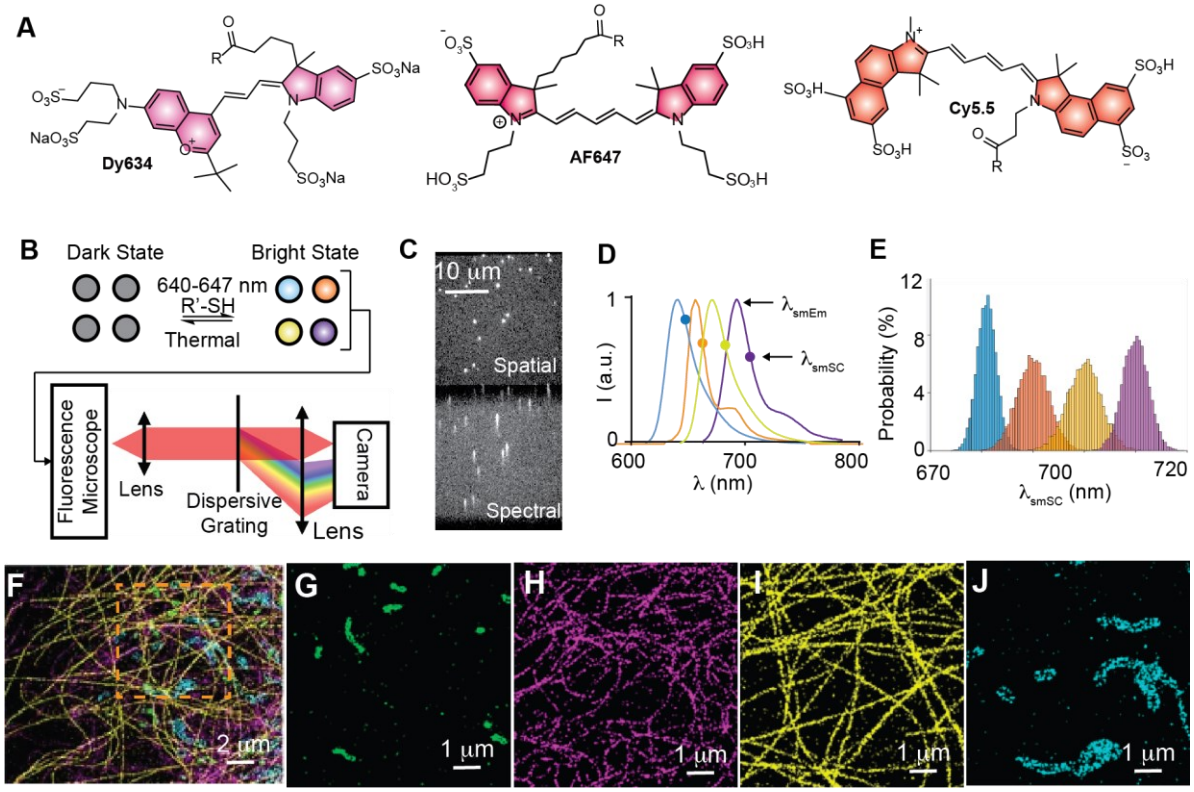

Fig. 1. (**A**) Representative molecular structures of far-red photoswitchable cyanine dyes for multiplexed sSMLM; R in dye structures indicates the labeling site to attach biomolecules. (**B-E**) Concept of parallel multiplexed sSMLM: (**B**) a set of photoswitchable fluorophores (shown as blue, orange, yellow and purple circles) can simultaneously photoswitch under similar imaging condition; their single-molecule emission signals are captured by a typical fluorescence microscope coupled with a dispersive element (grating shown as an example) to provide spatial and spectral images (**C**) of every single molecule; simulated emission spectra (**D**) and histogram of λ_{smSC} probability distributions (**E**) of four hypothetical far-red photoswitchable fluorophores demonstrate the concept of single-molecule spectral discrimination based on statistically resolved λ_{smSC} distribution regardless of spectral overlaps with λ_{smEm} separations about 10 nm; (**F-J**) Representative four-color simultaneous multiplexed sSMLM overlayed image (**F**) in a PtK2 cell with its peroxisome (**G**), vimentin (**H**), tubulin (**I**), mitochondria (**J**) structures separately displayed and labeled with Dy634, DL650, CF660C, and CF680, respectively Images in **F-J** is adapted with permission from *Ref.* 18, Copyright 2015 Springer Nature.

buffer (referred to as GLOX) system to yield high-quality "single-molecule blinking" events with photon budgets up to ~10^4 (**Fig. 1B** top).[18,41]

The bottom part of **Fig. 1B** shows the concept of a representative sSMLM systems. Briefly, the single-molecule emission signals are collected using a conventional fluorescence microscopy system with a high-magnification (60-100×) objective lens. The emission signals are then passed through a dispersive element (e.g. grating or prism) to provide both spatial and spectral images (**Fig. 1C**) of individual molecules using relay optics. A camera with single-molecule sensitivity [e.g., electron-multiplying charge-coupled device (EMCCD) or scientific complementary metal oxide semiconductor (sCMOS)] is used to capture both images for single-molecule localization, spectral discrimination, and subsequent multi-color sSMLM imaging reconstruction. Both grating- and prism-based imaging spectrometer designs have been implemented for sSMLM. The existing grating-based spectrometer is relatively compact and experiences minimal aberrations while its transmission efficiency is relatively low (~70%).[23] On the other hand, a prism-based spectrometer has higher transmission efficiency but more complications in system alignment and it may have aberration/distortion correction as it employs either separate focusing lenses or beam paths.[24] In addition, the prism offers a relatively nonlinear wavelength-pixel relationship, while the grating provides a linear wavelength-pixel relationship.

Since the full emission spectra (**Fig. 1D**) of individual fluorophores are captured using sSMLM, the single-molecule emission peak (λ_{smEM}) or the intensity-weighted spectral centroid (λ_{smSC}) can be calculated to discriminate the fluorophores. However, only maximally four fluorophores have been demonstrated for their simultaneous imaging with > ~95% molecular identification accuracy due to the single-molecule spectral variations observed from the same fluorophore species.[18] These spectral variations originated from both intrinsic single-molecule fluorescence spectral heterogeneity (smFSH)[39] and noise uncertainty in the single-molecule spectral detection process.[42] The collective spectral variations are typically quantified by calculating the standard deviation (σ) of λ_{smEM} or λ_{smSC} distribution from ~10^5-10^7 single molecules of a pure fluorophore sample across different imaging field of view (FOV). A hypothetical example of a set of four fluorophores with λ_{smEm} separations about 10 nm from each other and σ values of ~3 nm allows the differentiation of the four fluorophores statistically (**Fig. 1E**).

The Xu group reported a seminal four-color sSMLM experiment that images the peroxisome (green), vimentin (magenta), tubulin (yellow), and mitochondria (cyan) in a fixed PtK2 cell (**Fig. 1F**). Its subcellular organelle marker proteins for these structures are respectively labeled with Dy634, Dylight 650, CF660C and CF680.[18] These four cyanine fluorophores have relatively low σ values for the spectral variations (~1.5-4.5 nm)[18,39] [39] We summarized the key ensembled and single-molecule photophysical parameters and imaging buffer conditions to operate these simultaneous photoswitchable fluorophore sets in **Table 1**. Four different dye-tagged secondary antibodies orthogonally targeting the corresponding primary antibodies raised from four different species (*i.e.,* mouse, rabbit, chicken, and rat) to achieve simultaneous multi-color labeling. The green, magenta, yellow, and cyan channel exclusively showed cluster-like, fibrous, linear, and worm-like structures which agree with the morphologies of the four aforementioned organelles, demonstrating the highly multiplexed imaging capability of sSMLM (**Fig. 1G-J**). Several two or three-color sSMLM experiments and ratiometric spectral detection with dichroic filters have also been reported using the combinations of AF647, CF660C, and CF680. [23,40,43]

Synthetic photoswitchable fluorophore sets for multiplexed FL-SMLM imaging

A set of photoswitchable fluorophores can also be utilized to achieve multi-color mSMLM by distinguishing their single-molecule fluorescence lifetime (τ_f) distributions. For instance, Enderlein et al reported the use of two classical red photoswitchable fluorophores **Cy3B** and **ATTO550** (**Fig. 2A**) to achieve two-color FL-SMLM imaging.[27] The selection of the fluorophores exploits multiple fluorophore families (*e.g.,* Cyanines, Rhodamines) which encode distinct fluorescence lifetimes. Specifically, a HeLa cell was labeled with the two dyes and imaged using the phosphate buffer saline with 500 mM NaCl. A representative fluorescence-lifetime color-coded FL-SMLM image is shown in the top part of **Fig. 2B**. The distinct morphologies (elliptical mitochondria and cluster-like peroxisome) are illustrated in the orange and green channels, respectively. Two distinct populations in the histogram of τ_f distribution (**Fig. 2B** bottom) from the images further

Table 1. Ensembled and single-molecule photophysics of photoswitchable fluorophore for simultaneous multiplexed sSMLM

Fluorophore	λ_{abs} (nm)[a]	λ_{smEm} (nm)[b]	λ_{smSC} (nm)[c]	σ (nm)[d]	Buffer	$\lambda_{Ac}/\lambda_{Ex}$ (nm)
mEOS 4b	570	580	-	-	GLOX /bME[e]	405/532
PAmKate	586	600-625	-	5.4	-	405/561
PAmCherry	564	595	-	6.0	-	405/561
Dendra2	553	590-620	-	5.7	-	405/561
Dy634	635	664	681	1.9	GLOX /MEA[f]	-/640-647
AF647	651	670	686-690	2.1	GLOX /MEA	-/640-647
Dylight 650	650	672	690	3.1	GLOX /MEA	-/640-647
CF660C	667	688	695-700	3.1	GLOX /MEA	-/640-647
Cy5.5	683	697	701	3.5	GLOX /MEA	-/640-647
CF680	681	704	706-710	2.2	GLOX /MEA	-/640-647

[a] Values obtained from Thermofisher SpectraViewer, FPbase.org, and Biotium; [b] averaged single-molecule emission peaks; [c] averaged intensity-weighted single-molecule spectral centroid; [d] standard deviation value of single-molecule spectral peak or centroid variations; [e-f] GLOX buffer consists of Catalase, Glucose and Gluocose Oxidase in Tris HCl with [e] 143mM β-mercaptoethanol (βME) or [f]100-1000mM mercaptoethylamine.

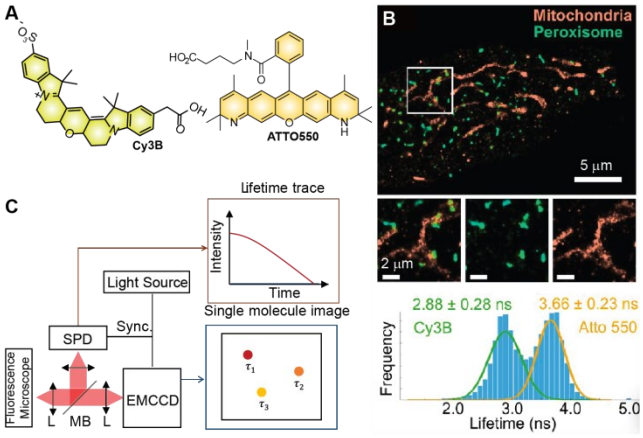

Fig. 2. (**A**) A representative pair of photoswitchable fluorophores **Cy3B** and **ATTO550** used for simultaneous FL-SMLM imaging ; (**B**) top: FL-SMLM images of a fixed HeLa cell labeled with Cy3B (green) and Atto550 (orange); bottom: Histogram (bars) and double Gaussian fitting (green and orange curves) of the fluorescence lifetime distributions of Cy3B and ATTO550 measured in the HeLa cell. (**C**) A schematic illustration of an FL-SMLM system; L: lens; MB: magnetic base; Images in **B** were adapted with permission from *Ref.* 27, Copyright 2022 American Chemical Society

indicated the differences in τ_f (2.88 ns for **Cy3B** and 3.66 ns for **ATTO550**) and validated the multiplexing capability in FL-SMLM using τ_f resolvable photoswitchable fluorophore sets. AF647 (τ_f = 1.51 ns)/ATTO655 (τ_f = 3.42 ns) have also been demonstrated as a pair of simultaneous photoswitchable fluorophores for FL-SMLM imaging.[28]

Instrumentation-wise, FL-SMLM combines the spatial resolution of single-molecule localization microscopy (SMLM) with the temporal information provided by fluorescence lifetime imaging microscopy (FLIM).[27,28] Practically, two detection channels, are switched by flipped optics using the magnetic base (MB); the spatial information of the emitted molecules is captured by the EMCCD camera while their temporal information is obtained by a single-photon detector (SPD) in another emission beam path with a synchronized light source and detectors (**Fig. 2C**). These two pieces of information can be simultaneously obtained using a beam-splitting configuration and the lifetime trace can be used as a signature of the individual molecules.

Photoswitchable fluorescent protein sets for multiplexed sSMLM imaging

In addition to the use of simultaneous photoswitchable synthetic fluorophores, multi-color sSMLM experiments have also been achieved using photoactivatable/photoconvertible proteins[19,22] (mEOS 4b, PamKate, PamCherry, and Dendra2). Their photophysical parameters are also listed in **Table 1**. The elevated σ value, relatively low photon budget, and the need for an activation wavelength (λ_{Ac}) for the photoconvertible proteins complicate the multiplexing capability and result in elevated single-molecule misidentification.[19,22] However, unlike the photoswitchable dyes that often require immunofluorescence labeling, the fluorescent proteins can be transiently or stably expressed in cells, which is beneficial for live-cell imaging of biomolecular interactions.

In sum, the development of simultaneous photoswitchable fluorophore sets paired with sSMLM and FL-SMLM optical systems has allowed the parallel, multiplexed mSMLM imaging of subcellular structures and protein interactions in fixed and live cells independent of the emission spectral overlap of the fluorophores. These simultaneous multiplexed mSMLM imaging capabilities would be particularly valuable for the investigation of complex nanoscopic interactions and colocalizations among individual biomolecules (proteins, DNAs) and subcellular organelles (mitochondria, lysosome, chromatin) which have a profound impact on fundamental molecular processes in life processes.[38]

Polarity-sensitive and switchable fluorophores for nanoscale polarity and hydrophobicity mapping

PAINT-based SMLM imaging method does not require the exploit of photoswitchable fluorophores.[44] Instead, fluorophores that can transiently bind to the substrate in a millisecond time scale permit the operation of stochastic single-molecule fluorescence switching and subsequent SMLM imaging scheme. Bridging PAINT and sSMLM into sPAINT imaging, several studies demonstrate the utility of polarity-sensitive and transient-binding-based switchable fluorophores for mSMLM imaging towards nanoscale polarity and hydrophobicity mapping. This is because sSMLM/sPAINT can capture minute single-molecule spectral responses of the same fluorescent probes at different local environments.[7–9]

Polarity-sensitive Nile Red (NR) and its derivatives have extensively been exploited for sPAINT. Danylchuk et al developed **NR12S**, **NR12A**, and **NR4A** to target cell membranes (**Fig. 3A**).[10] The attachment of short alkyl chains in **NR4A** allows its transient interaction with the cell membrane for live-cell sPAINT imaging (**Fig. 3B**). sPAINT imaging of **NR4A** depicts ordered and smooth lipid bilayers (blue) and observes 200-nm membrane pits with lower lipid order and red-shifted NR4A spectra in the arrow-pointed areas (**Fig. 3C**). Longer alkyl chains in **NR12A** resulted in stronger binding to the plasma membrane and can be used as a conventional fluorescence microscopy membrane stain.

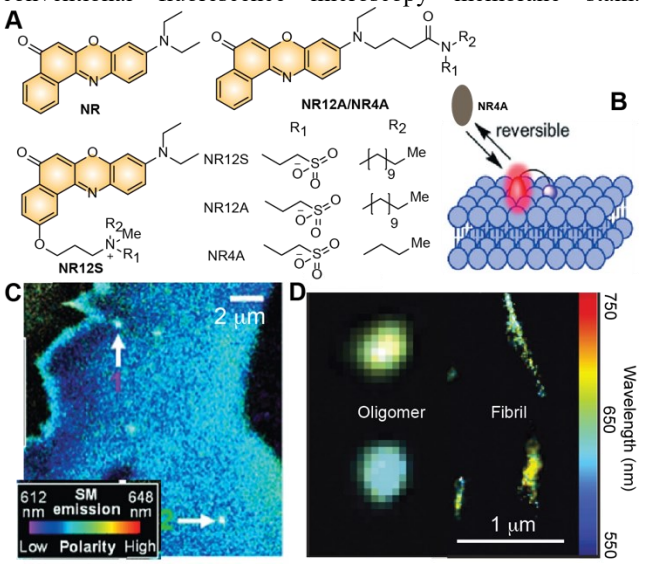

Fig. 3. (**A**) Structures of NR and its derivatives designed for superresolution polarity and hydrophobicity mapping using sPAINT; (**B**) Principle of sPAINT with **NR4A**: the single-molecule fluorescence blinkings signals are generated by the transient interactions between **NR4A** and the lipid bilayers; (**C**) an sPAINT image of a live COS-7 cell with the λ_{smEm} changes on the cell membranes; the arrow-pointed area in **C** highlights the observed pits with significant bathochromic shifts in λ_{smEm} compared with those detected in the membrane; (**D**) an sPAINT image of individual aβ oligomers and fibrils. Images in **C** and **D** were adapted with permission from *Ref.* 10, Copyright 2019 Wiley-VCH, and *Ref.* 8, Copyright 2016 Springer Nature, respectively.

Bongiovanni et al reported the nanoscale hydrophobicity mapping of amyloid-β (aβ) protein misfolding related to Alzheimer's disease by capturing the distinct spectral shifts of NR upon binding to the aβ protein aggregate (**Fig. 3D**).[8] Depending on the protein aggregation status (Oligomers vs. Fibrils), sPAINT can capture significant spectral changes (600 nm to 635 nm) of NR which indicates the altered hydrophobicity. A few studies have then reported the super-resolution polarity mapping in cells[7,10] and biomaterials[9,11] using similar approaches.

In short, taking advantage of polarity-responsive switchable fluorophores, sSMLM reveals nanoscale polarity and hydrophobicity changes in protein aggregates, cell membranes, and self-assembling nanocarriers for the first time, opening up the era of functional super-resolution microscopy.[45] Such nanoscale polarity imaging would permit the understanding of various alternations in lipid compositions and cell membrane functions/integrity and other polarity/hydrophobicity changes in the subcellular environment that would potentially be associated with the pathogenesis of the disease.[29]

Orientation-sensitive and switchable fluorophores for SMOLM

SMOLM is a recently emerged nanoscale imaging technique based on mSMLM to visualize the nanoscale orientational organizations of biological structures.[16] Single-molecule dipole moments or orientations have been extensively studied[46,47]. SMOLM further pushes the capability of single-molecule orientation imaging towards the super-resolution mapping in crowd biological samples taking advantage of switchable fluorophores coupled with high-sensitivity fluorescence polarization detection of individual probe molecules. Particularly, SMOLM concurrently localizes the position of individual molecules and determines the orientational information of individual switchable probe molecules. This is accomplished by analyzing the fluorescence polarization of the emitted light from each molecule, which provides information about the orientation of the fluorophore relative to the microscope's polarization axis.

To achieve optimal SMOLM imaging, it is critical to identify orientation-sensitive fluorophores for the compositions of the substrates of interest.[16,26] For instance, **DiI** is a classical cell membrane marker with a well-known parallel orientation to the supported lipid bilayers (SLB) consisting of gel-phase Dipalmitoylphosphatidylcholine (DPPC) while **MC540** can switch from a perpendicular orientation with respect to the fluidic lipid membrane to a parallel orientation in cells (**Fig. 4A**). **Fig. 4B** illustrates the simplified and representative schematics of the SMOLM systems to capture the molecular orientation.[16] The system includes a polarization-splitting module in the emission beam path, and after the intermedial image plane, relay optics, and a polarizing beam splitter (PBS) are used to split the emission into two different polarization directions, which are then captured by separate cameras. Manipulating all the pixels of the phase mask at the back focal plane (BFP) allows the encoding of the 3D positions and 3D orientation of the molecules.[15]

Lew et al recently reported the six-dimensional SMOLM imaging (x, y, z, rotational angles ϕ and θ, and wobble angle Ω) of single MC540 molecules in a fixed HEK293T cell (**Fig. 4C**).[15] The colors in **Fig 4C** represents the differences in azimuthal angles of each **MC540** molecule relative to the cell

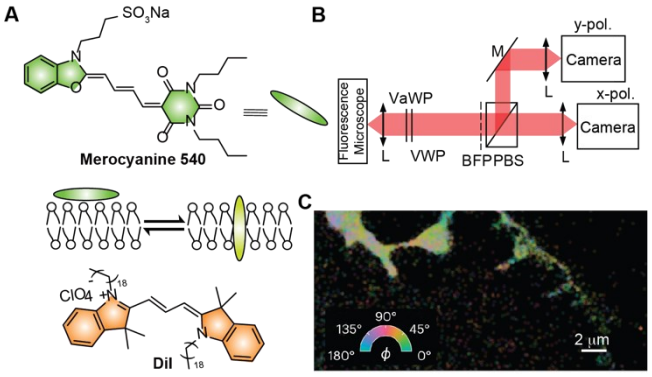

Fig. 4. (**A**) Structures of orientation-sensitive fluorophores **MC540** and **DiI** and an illustration of the fluorophore orientation changes from parallel to perpendicular when interacting with lipid bilayers; (**B**) Simplified optical detection scheme for SMOLM; VaWP: Variable wave plate; VWP: Voltex wave plate; BFP: back focal plane; PBS: polarizing beam splitter; (**C**) A presentative SMOLM image of a fixed HEK-293T cell imaged that were color-coded by the detected azimuthal angles (ϕ) of each single **MC540** molecule. Image in **C** was adapted with permission from *Ref.* 15, Copyright 2022 Springer Nature.

membrane which agrees well with the SMOLM measurement on SLB. It was also found that NR (**Fig. 3A**) has a great orientational sensitivity to image lipid-containing cholesterol[16] and αβ42 protein aggregates[15]. Furthermore, Rimoli et al reported a 4polar-STORM method for the super-resolution mapping of orientations of dye-labeled actin filaments using 2D orientation to infer 3D orientation of the probes.[26] A photoswitchable Alexa Fluor 488 probe is covalently attached to Phallodin to label the actin with a rather immobilized geometry along the actin fiber axis to enable orientation imaging.[26]

Notably, since most of the fluorophores are considered as dipole-like emitters with intrinsic fluorescence anisotropy/polarization features, all SMLM-compatible dyes can be, in principle, exploited for SMOLM imaging. However, the compositions of the substrates of interest (e.g., different lipids) and the fluorophore binding modes to the substrates to reduce orientational flexibility should be investigated to facilitate high-quality SMOLM imaging. SMOLM would potentially provide invaluable insights into the molecular orientation or rotational dynamics in probing diverse biomolecular interactions such as protein-protein, protein-DNA, and protein-lipid interacting patterns.

Bright and switchable fluorophores for fast single-molecule diffusivity mapping

SM*d*M allows researchers to reconstruct super-resolution maps of fast diffusing dynamics of individual molecules within live biological systems.[13,14,48] By tracking the movement of individual molecules over a short period of time, (<=1 ms) using stroboscopic illumination (**Fig. 5A**)[12], SM*d*M enables the mapping of single-molecule diffusion coefficient around 20-30 $\mu m^2/s$ that would otherwise be impossible to achieve using other dynamics monitoring methods (e.g., Fluorescence Recovery After Photobleaching or Fluorescence Correlation Spectroscopy). More specifically, the two excitation pulses are placed towards the end of the first frame and the beginning of the second frame to achieve a center-to-center time separation between the two recorded images as short as 1 ms (**Fig. 5A**). Noting that the camera exposure time remains at 9.1 ms to capture single-molecule images.

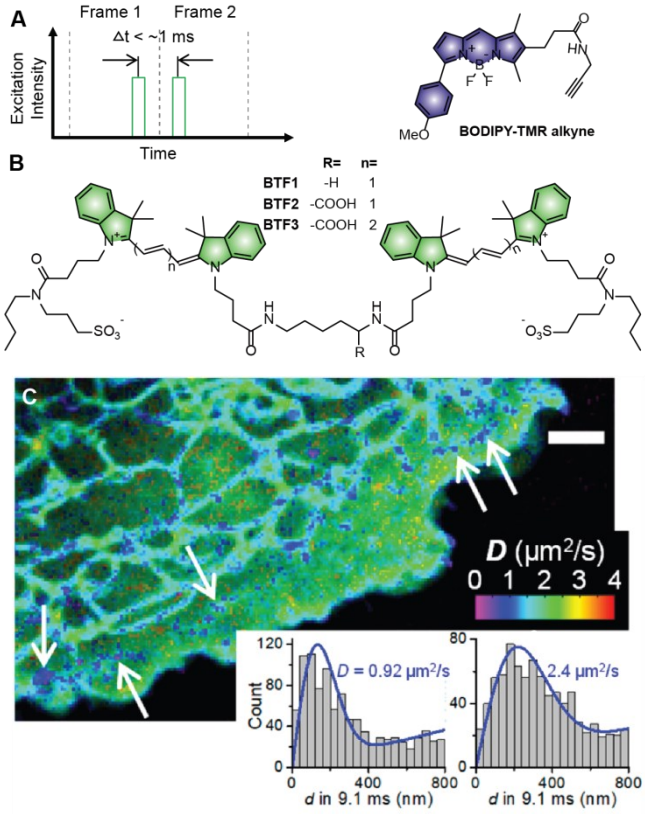

Fig. 5. (**A**) The concept of stroboscopic illumination for SM*d*M which excites the fluorophores using paired pulses of stroboscopic illumination, synchronized with the camera acquisition; (**B**) Structures of SM*d*M fluorophores **BTF1-BTF3** and **BODIPY-TMR alkyne**; (**C**) A representative SM*d*M image of a live COS-7 cell using **BODIPY-TMR alkyne;** arrows indicate the nanodomains with lower diffusivity; inset in **C** shows the distributions of single-molecule displacements for the nanodomains (left) and other parts of the plasma membrane (right) together with the maximum-likelihood fitttings for diffusivity distributions. Images in **C** were adapted with permission from *Ref.* 14, Copyright 2020 American Chemical Society

SM*d*M has used classical photoswitchable fluorescent proteins such as mEos3.2[12] and Dendra2[48] to image live cells and photoswitchable dye AF647 and Cy3B to image protein charges[48] and enzymes[13] respectively. Recently there are a few switchable and functional fluorophores specifically developed or screened for SM*d*M. For instance, Klymchenko et al developed fluorogenic dimers (**BTF1-3**, **Fig. 5B** bottom) based on Cyanine dye design.[31] These fluorophores are in the non-emissive state due to H-aggregation-induced fluorescence quenching in an aqueous solution and switched to emissive states when reversibly bind to the lipid membranes. Owing to its higher photon budget (~3-fold increase than **NR**), it allows SM*d*M mapping of intramembrane diffusion coefficient with a 10-fold reduced diffusion coefficient compared with the measurement in **NR**, presumably due to the dimeric structure of the probes with a high length of the molecule in the open form.

Another commercially-available small switchable organic fluorophore (**BODIPY-TMR-Alkyne, Fig. 5B** top) has been used to unveil the nanoscale membrane diffusivity heterogeneity of cellular membranes.[14] This probe has an outstanding fluorescence quantum yield (95%) and shows a fluorescence on-off switching feature upon binding to the cell membrane to generate single-molecule blinking with a photon budget of ~1000 within 1-ms excitation or 2-fold brighter than that of NR measured at the same imaging condition. The measured diffusion coefficient using **BODIPY-TMR alkyne** (~2.2 μm^2/s) is comparable to those previously measured from single-molecule tracking experiments. Using this switchable fluorophore, Xu et al reported the SM*d*M mapping of cellular membranes. Particularly, the endoplasmic reticulum (ER)-tubule membrane (cyan) shows a lower diffusivity than those of the plasma membrane (green) (**Fig. 5C**). Nanodomains forms after the treatment of the cell with cholera toxin B subunit with significant lower diffusivity (arrow-pointed regions and inset of **Fig. 5C**).

The capability of SM*d*M has been pushed to probe the ultrafast diffusions (up to 300 μm^2 s^{-1}) of small solutes or dye molecules (molecular weight < 1 Kilodalton)[49] with the careful selection of dyes that have unhindered mobility in the cytoplasm. Many existing fluorophores face a dilemma for ultrafast SM*d*M monitoring as typical cell-permeable organic small fluorophores are rather hydrophobic and tend to interact with the lipid structures which hinder diffusion. Reversely, introducing hydrophilic groups (e.g., sulfonate) would likely prevent its penetration into the cell. Xu et al devised a graphene-based in situ electroporation technique to deliver hydrophilic and otherwise cell impermeable dyes (e.g., **Cy3B** and **AF647**) to the cytoplasm to probe unhindered diffusions of the cytoplasm[49] In sum, SM*d*M allows the super-resolution mapping of fast dynamic events in live cells and materials using cellularly diffusion-unhindered switchable and bright fluorophores, shedding light on the mobility and intracellular transport of proteins and small biomolecules and helping to elucidate the mechanism of trafficking and diffusion process in cells.[12]

Challenges and outlook on fluorophores design and integration with optical implementation and imaging processing methods for mSMLM

Fluorophores' Single-Molecule Heterogeneity in mSMLM

As a classical observation in any single-molecule studies, single-molecule fluorescence heterogeneity is often observed in mSMLM experiments in spectral and lifetime domains which partially account for the broadening of the histogram as illustrated in **Fig. 1E** and **2D**. It has been hypothesized that the origin of such heterogeneity is associated with the conformational changes of the chromophores coupled with or affected by the physical or chemical properties of the local environments.[4] The understanding of the origins and the engineering of fluorescence heterogeneity is the key to unleashing the capability of mSMLM.

sSMLM not only benefits from the development of low-heterogeneity fluorophores but also facilitates the study of such origins of smFSH with its high-throughput single-molecule fluorescence spectroscopy function.[39,50,51] Kim et al reported the investigation of trans-cis isomerizations of a **Merocyanine** using sSMLM (**Fig. 6A**).[51] Specifically, they immobilized a Spiropyran molecule on a poly-D-Lysine coated glass substrate and use a 405-nm laser to promote ring-opening reaction from the spiropyran to the merocyanine form. The sample is filled with different organic solvents and the merocyanine form is excited with a 561-nm laser. They observed two distinct spectral populations with similar photon budgets (**Fig. 6B**). The ratio of detected **TTT** isomer versus **TTC** isomer (structure shown in **Fig. 6A**) was found to be

inversely proportional to the increase of solvent polarity (**Fig. 6C**) which is consistent with the predicted differences in dipole moments of **TTT** and **TTC** using density functional theory (DFT).

We recently reported the observations of four different conformational isomerizations of Boron Dippyrolemethne (BODIPY) chromophores (**Fig. 6D**).[50] Particularly, the two single-bond flanked by the ethylene bridge between the benzoxazole/benzothiazole and the BODIPY core can both adapt trans and cis configurations. In addition, By correlating with time-dependent DFT (TDDFT) simulations, we found that the blue-shifted distinct spectral populations detected by sSMLM originated from **TTT** and **TTC** isomers of the BODIPY chromophores while the red-shifted populations are from **the CTC** and **CTT** isomers. Presumably, all these isomerizations and conformational changes have much faster kinetics in ensembled solution measurement, which may slow down due to the immobilization of the molecules on the substrates.

Furthermore, we observed a counter-intuitive phenomenon that rigid chromophores such as Rhodamine 101 and Pentacene still have significant large single-molecule fluorescence spectral heterogeneity (smFSH, σ = 6.7 nm and 9.0 nm respectively) compared with that of a Cyanine-based dye AF647 (σ = 3.3 nm) (**Fig. 6F-H**). Cyanine dyes are known for their flexible conformations due to the flexible polymethine bridge. The origins of the smFSH remain unclear and it is critical to investigate the fluorophore-substrate interactions to design next-generation fluorophores for mSMLM. We discussed the several aspects of fluorophore designs for mSMLM below including the engineering of fluorophores' single-molecule heterogeneity.

Minimizing single-molecule fluorescence heterogeneity for parallel, hyperplexed mSMLM

Despite several studies reporting simultaneous multiplexed sSMLM or FL-SMLM imaging, the number of color channels or resolvable fluorescence labels is limited to four in a single far-red spectral channel (~650-800 nm). The major challenges towards mSMLM towards hyperplexed imaging (>10 colors) are mainly from the photophysical and photochemical properties of the fluorophores. The spectral variations of currently used fluorophores for multiplexed sSMLM range from ~2-6 nm ($\sigma_{smSC}/_{smEm}$, **Table 1**) which are both influenced by smFSH and spectral precision[23] of the imaging system.

New strategies for minimizing smFSH of photoswitchable fluorophores would allow for resolving more fluorophores in the fixed codespace (visible spectral region of 400-800 nm) using their high-dimensional spectral signatures in a conventional fluorescence microscope. Similar concepts can be extended to FL-SMLM to narrow down the fluorescence lifetime distributions, thus enhancing its multiplexing capability. Understanding the interplay of inhomogeneous chromophore-environment interactions in the dimension of interest that fundamentally underlines the single-molecule heterogeneity will shed light on fluorophore engineering strategies.[52] Presumably, novel environmental insensitive chromophore structures with different functional groups encoding different net charges (e.g. sulfonate, polyethylene glycol chains, ammonium salts) need to be explored to minimize single-molecule fluorescence heterogeneity for hyperplexed mSMLM.

Fluorescent probes engineering for functional mSMLM

In mSMLM functional imaging, the fluorophores probe the distinct local environmental properties such as different domains in lipid, and parallel vs. perpendicular orientations of fluorophores in the cell membrane. Despite the great premise of functional mSMLM, only a few dimensions have been investigated and exploited so far to probe predominantly two distinct phases of the substrates. Expanding the capability of functional imaging requires the identification of switchable fluorescent probes that can (1) generate stochastic single-molecule fluorescence switching for localization and (2) show large and distinct changes in their fluorescence profiles in the respective dimensions of interest. The former challenges could be largely addressed using PAINT-based SMLM imaging strategies while the latter might benefit from revisiting the extensively reported fluorescent sensors[53–55] for analyte detection in the ensemble measurement.

The nature of intricate biological systems would be highly benefited from the probing of multiple functions to comprehend the coordination of different pieces of the complex biomolecular machinery. The fluorescent probe

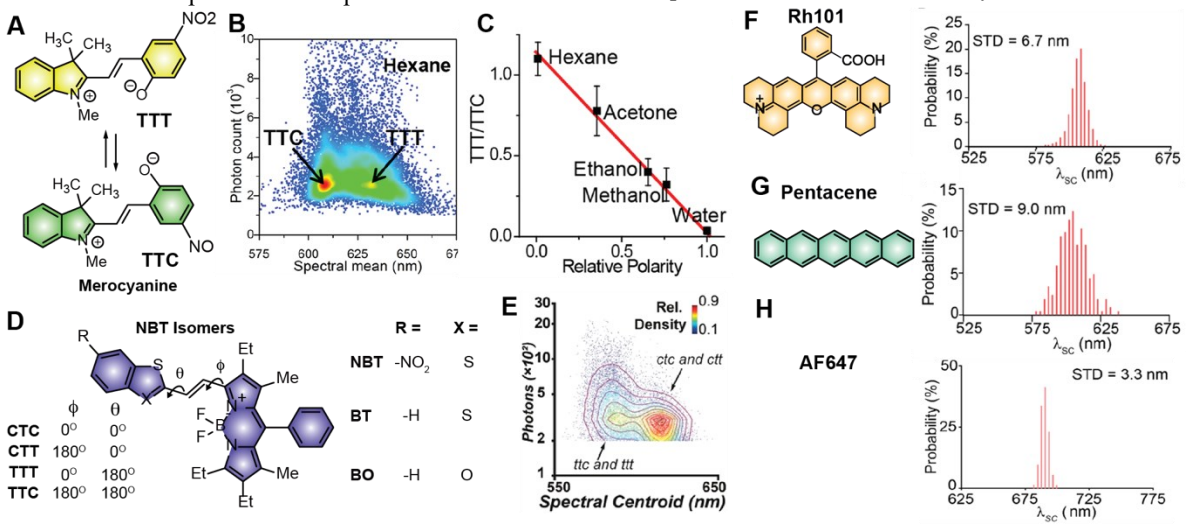

Fig. 6. (**A-C**) Structures (**A**) of **TTT** and **TTC** isomers of a **Merocyanine** chromophore; (**B**) distinct λ_{smSC} populations were observed for the **Merocyanine** TTC and TTT isomers; (**C**) A plot shows the solvent-dependent ratios of the **TTT** versus the **TTC** isomers; (**D**) Structures and four conformational isomers observed using sSMLM; (**E**) a representative scatterplot shows two distinct λ_{smSC} populations of BODIPY chromophores from the *ttt* and *ttc* versus *ctc* and *ctt* isomers. (**F-H**) Histogram of λ_{smSC} probability distributions of Rh101 (**F**), Pentacene (**G**) and AF647 (**H**) respectively; **B-C** were adapted with permission from *Ref.* 51, Copyright 2017 American Chemical Society, **E** was adapted with permission from *Ref.* 50, Copyright 2019 American Chemical Society, and **F-H** were adapted with permission from Ref. 39, Copyright 2021 American Chemical Society, respectively.

designing strategies to detect multiple states are the key to multi-functional mSMLM. For example, NR has been demonstrated to be one of such ideal probes that can sense the local polarity as well as the orientations of lipids. The optical integration of different mSMLM imaging modalities would allow the decoding of these functions simultaneously. Furthermore, in intricate biological systems, many substrates might have more than two phases, and designing strategies to probe multiple phases or states at the nanoscopic level would allow a better understanding of multi-functional biological systems.

Even higher photon budgets are desired for mSMLM

In mSMLM, the relatively low SNR using existing switchable fluorophores is inevitable due to the split and dispersion of the single-molecule emission signals to obtain additional information other than spatial coordinates.[16,23] However, a high SNR is crucial for high-precision multidimensional single-molecule detection. Therefore, a higher photon budget is desired from the dye perspective.

New fluorophore design strategies to enhance the photon budget would be the key to maximizing the capability of mSMLM. The introduction of triplet-state quenchers and oxygen depletion reagents in the solution of the sample is typically used to increase the photon budget and suppress photobleaching.[56] Second, the DNA-PAINT-based imaging approach significantly increases the photon budget by programming the binding kinetics between a fluorophore-labeled imager strand and a biomolecule-labeled docking strand.[57] Longer single-stranded oligonucleotides provide extended binding and thus generate long-lasting single-molecule blinkings at the expense of slowing down imaging acquisition.[58] Third, from a fundamental ensemble photophysics point of view, the brightness of fluorophore is equal to the multiplication of the fluorescence quantum yield and the molecular absorption coefficient.[59] However, for single-molecule photophysics, the fluorophores are predominantly staying in the excited state above the so-called "saturated excitation condition": because of the intense laser illumination. The photon budget is governed predominantly by the fluorescence quantum yield and triplet state lifetime.[60] Recently developed self-healing fluorophores[61,62] which covalently attach the triplet-state quencher to the chromophores and functional group engineering to suppress twisted intramolecular charge transfer[63] are prominent strategies to facilitate radiative decay, reduce triplet generation, and thus increasing the photon budget of the fluorophores.

Furthermore, the photoswitchable fluorophores often require different imaging buffers, excitation & activation laser illumination schemes, and triplet state quenchers to induce bright single-molecule blinkings case by case. In order to achieve simultaneous multiplexed mSMLM imaging, it is desired to design strategies that allow simultaneous photoswitching of a broad spectrum of fluorophores with a brightness that allows single-molecule detection.

Lastly, the limited choice of orthogonal labeling strategies to label multiple biomolecules/substrates of interest is also a major bottleneck in multiplexed SMLM. Existing labeling strategies in mSMLM mainly used fluorophore-tagged antibodies18 and endogenously expressed fluorescent proteins and self-labeling peptides (e.g., SNAP-tag and HaloTag).[35] The simultaneous high-quality labeling of multiple biomolecules within the same cell is challenging due to the variations in antibody affinity and transfection efficiencies. New strategies to develop small-molecules and peptide-based targeting ligands conjugated with switchable fluorophores to label different biomolecules directly would be beneficial.

Better utilizing photons in imaging collection/detection path for mSMLM

Synergistically, better optical strategies for more efficiently utilizing the precious photon budget are also needed to advance mSMLM. As an example, in sSMLM, a compact monolithic imaging spectrometer using a dual wedge prism (DWP) was introduced for better sSMLM imaging.[24] This DWP-based imaging spectrometer is a single unit of optics based on a wedge prism pair, which minimizes the transmission loss caused by either a grating or a series of optics in the emission beam path, resulting in improved localization precision. Sophisticated optical configurational techniques, such as 4pi-SMLM,[64] or modulation-enhanced SMLM (meSMLM – repetitive optical selective exposure (ROSE)[65]; structured illumination-based point localization estimator (SIMPLE)[66] can be incorporated into the existing mSMLM to better collect or utilize the limited fluorescence emission signals. These advancements in optical instrumentation will be able to not only improve the mSMLM's accessibility from researchers in diverse fields but also accelerates the mSMLM imaging performance.

Machine learning-based imaging analytics

Additionally, it is vital to develop advanced imaging analysis methods for mSMLM. The mSMLM imaging data contain multidimensional molecular information and are often complex and difficult to interpret. Innovative machine learning-based imaging analysis methods provide invaluable tools for decoding mSMLM data. In SMLM, machine learning algorithms have been exploited to detect and localize individual molecules in each frame in the SMLM video sequence[67–69], to perform background estimation and subtraction[70], and to speed up super-resolution maps of cellular structures at the post-reconstruction stage.[71] These strategies can further be extended to mSMLM. For example, multiple strategies have reported the development of convolutional neural networks (CNN) to reduce the misidentification rate among different fluorophores in sSMLM using raw spectral images up to 10 times compared with the identification based on discriminating λ_{smSC}.[38] Presumably, the unprocessed images contain high-dimensional features that provide additional information for classification and can only be recognized by machine learning neural networks.

Beyond adopting existing machine learning methods in SMLM for the acceleration of single-molecule functional information extraction, improving precisions of functional measurement, background estimation, feature extraction, object detection, semantic segmentation, etc. New neural network architectures such as transformer-based feature networks[72] and transfer learning[73] might potentially outperform CNN-based neural networks. On the other hand, as many real SMLM experiments do not have ground truth, it is also critical to develop new physical-informed simulation approaches as the ground truth for the training and validation of developed neural networks.

Conclusion

In summary, we provided our perspective on the frontier development in the emerging field of mSMLM with an emphasis on the fluorophore designs tailored for each mSMLM modality. We highlighted intriguing examples in simultaneous multiplexed super-resolution imaging using simultaneous photoswitchable fluorophore sets coupled with sSMLM and FL-SMLM. We further discussed the use of polarity-sensitive, orientation-sensitive, and bright switchable fluorophores for functional nanoscale mapping of local polarity/hydrophobicity, orientation, and diffusions paired with sPAINT, SMOLM, and SM*d*M imaging systems, respectively.

We further discussed the current challenges and future outlooks, once again, from the synergistic developments of fluorescent probe design, the optical imaging method, and imaging analysis to fully unleash the power of mSMLM. We envision that multidisciplinary efforts and collaborations from dye chemistry, chemical biology, optical imaging method, imaging processing, and many other related fields will greatly promote the development of mSMLM toward decoding molecular functions and interactions in the structurally and dynamically complex biological environments and life processes.

AUTHOR INFORMATION

Corresponding Authors

Yang Zhang - Molecular Analytics and Photonics (MAP) Laboratory, Department of Textile Engineering, Chemistry and Science, North Carolina State University, Raleigh, NC 27606, USA. Email: yang.zhang@ncsu.edu**.**

Ki-Hee Song – Quantum Optics Research Division, Korea Atomic Energy Research Institute, Yuseong-gu, Daejeon 34057, Republic of Korea. Email: songkihee@kaeri.re.kr**.**

Notes

The authors declare no competing financial interest.

ACKNOWLEDGMENT

This work was supported by the National Institutes of Health grants R21GM141675 and R01GM143397, the National Science Foundation grant CHM-1954430 and CHM-2246548, and the National Research Foundation of Korea grant No. NRF-2022R1C1C1002850.

References

(1) Rust, M. J.; Bates, M.; Zhuang, X. Sub-Diffraction-Limit Imaging by Stochastic Optical Reconstruction Microscopy (STORM). *Nat. Methods* **2006**, *3*, 793–796.

(2) Betzig, E.; Patterson, G. H.; Sougrat, R.; Lindwasser, O. W.; Olenych, S.; Bonifacino, J. S.; Davidson, M. W.; Lippincott-Schwartz, J.; Hess, H. F. Imaging Intracellular Fluorescent Proteins at Nanometer Resolution. *Science* **2006**, *313*, 1642.

(3) Jungmann, R.; Avendano, M. S.; Woehrstein, J. B.; Dai, M.; Shih, W. M.; Yin, P. Multiplexed 3D Cellular Super-Resolution Imaging with DNA-PAINT and Exchange-PAINT. *Nat. Methods* **2014**, *11*, 313–318.

(4) Moerner, W. E. Single-Molecule Spectroscopy, Imaging, and Photocontrol: Foundations for Super-Resolution Microscopy (Nobel Lecture). *Angew. Chem. Int. Ed.* **2015**, *54*, 8067–8093.

(5) Gustafsson, M. G. L. Nonlinear Structured-Illumination Microscopy: Wide-Field Fluorescence Imaging with Theoretically Unlimited Resolution. *Proc. Natl. Acad. Sci. U. S. A.* **2005**, *102*, 13081–13086.

(6) von Diezmann, A.; Shechtman, Y.; Moerner, W. E. Three-Dimensional Localization of Single Molecules for Super-Resolution Imaging and Single-Particle Tracking. *Chem. Rev.* **2017**, *117*, 7244–7275.

(7) Moon, S.; Yan, R.; Kenny, S. J.; Shyu, Y.; Xiang, L.; Li, W.; Xu, K. Spectrally Resolved, Functional Super-Resolution Microscopy Reveals Nanoscale Compositional Heterogeneity in Live-Cell Membranes. *J. Am. Chem. Soc.* **2017**, *139*, 10944–10947.

(8) Bongiovanni, M. N.; Godet, J.; Horrocks, M. H.; Tosatto, L.; Carr, A. R.; Wirthensohn, D. C.; Ranasinghe, R. T.; Lee, J.-E.; Ponjavic, A.; Fritz, J. V.; Dobson, C. M.; Klenerman, D.; Lee, S. F. Multi-Dimensional Super-Resolution Imaging Enables Surface Hydrophobicity Mapping. *Nat. Commun.* **2016**, *7*, 13544.

(9) Davis, J. L.; Zhang, Y.; Yi, S.; Du, F.; Song, K.-H.; Scott, E. A.; Sun, C.; Zhang, H. F. Super-Resolution Imaging of Self-Assembled Nanocarriers Using Quantitative Spectroscopic Analysis for Cluster Extraction. *Langmuir* **2020**, *36*, 2291–2299.

(10) Danylchuk, D. I.; Moon, S.; Xu, K.; Klymchenko, A. S. Switchable Solvatochromic Probes for Live-Cell Super-Resolution Imaging of Plasma Membrane Organization. *Angew. Chem. Int. Ed.* **2019**, *58*, 14920–14924.

(11) Park, Y.; Jeong, D.; Jeong, U.; Park, H.; Yoon, S.; Kang, M.; Kim, D. Polarity Nano-Mapping of Polymer Film Using Spectrally Resolved Super-Resolution Imaging. *ACS Appl. Mater. Interfaces* **2022**, *14*, 46032–46042.

(12) Xiang, L.; Chen, K.; Yan, R.; Li, W.; Xu, K. Single-Molecule Displacement Mapping Unveils Nanoscale Heterogeneities in Intracellular Diffusivity. *Nat. Methods* **2020**, *17*, 524–530.

(13) A. Choi, A.; H. Park, H.; Chen, K.; Yan, R.; Li, W.; Xu, K. Displacement Statistics of Unhindered Single Molecules Show No Enhanced Diffusion in Enzymatic Reactions. *J. Am. Chem. Soc.* **2022**, *144*, 4839–4844.

(14) Yan, R.; Chen, K.; Xu, K. Probing Nanoscale Diffusional Heterogeneities in Cellular Membranes through Multidimensional Single-Molecule and Super-Resolution Microscopy. *J. Am. Chem. Soc.* **2020**, *142*, 18866–18873.

(15) Zhang, O.; Guo, Z.; He, Y.; Wu, T.; Vahey, M. D.; Lew, M. D. Six-Dimensional Single-Molecule Imaging with Isotropic Resolution Using a Multi-View Reflector Microscope. *Nat. Photonics* **2022**, *17,* 179-186

(16) Lu J, Mazidi H, Ding T, Zhang O, Lew MD. Single-Molecule 3D Orientation Imaging Reveals Nanoscale Compositional Heterogeneity in Lipid Membranes. *Angew. Chem. Int. Ed.* **2020**, *59*, 17572-17579.

(17) Ding, T.; Wu, T.; Mazidi, H.; Zhang, O.; Lew, M. D. Single-Molecule Orientation Localization Microscopy for Resolving Structural Heterogeneities between Amyloid Fibrils. *Optica* **2020**, *7*, 602.

(18) Zhang, Z.; Kenny, S. J.; Hauser, M.; Li, W.; Xu, K. Ultrahigh-Throughput Single-Molecule Spectroscopy and Spectrally Resolved Super-Resolution Microscopy. *Nat. Methods* **2015**, *12*, 935–938.

(19) Dong, B.; Almassalha, L.; Urban, B. E.; Nguyen, T.-Q.; Khuon, S.; Chew, T.-L.; Backman, V.; Sun, C.; Zhang,

H. F. Super-Resolution Spectroscopic Microscopy via Photon Localization. *Nat. Commun.* **2016**, *7*, 12290.
(20) Song, K.-H.; Zhang, Y.; Brenner, B.; Sun, C.; Zhang, H. F. Symmetrically Dispersed Spectroscopic Single-Molecule Localization Microscopy. *Light Sci. Appl.* **2020**, *9*, 92.
(21) Butler, C.; Saraceno, G. E.; Kechkar, A.; Bénac, N.; Studer, V.; Dupuis, J. P.; Groc, L.; Galland, R.; Sibarita, J.-B. Multi-Dimensional Spectral Single Molecule Localization Microscopy. *Front. Bioinforma.* **2022**, *2*, 813494
(22) Mlodzianoski, M. J.; Curthoys, N. M.; Gunewardene, M. S.; Carter, S.; Hess, S. T. Super-Resolution Imaging of Molecular Emission Spectra and Single Molecule Spectral Fluctuations. *PLOS ONE* **2016**, *11*, e0147506.
(23) Zhang, Y.; Song, K.-H.; Dong, B.; Davis, J. L.; Shao, G.; Sun, C.; Zhang, H. F. Multicolor Super-Resolution Imaging Using Spectroscopic Single-Molecule Localization Microscopy with Optimal Spectral Dispersion. *Appl. Opt.* **2019**, *58*, 2248–2255.
(24) Song, K.-H.; Brenner, B.; Yeo, W.-H.; Kweon, J.; Cai, Z.; Zhang, Y.; Lee, Y.; Yang, X.; Sun, C.; Zhang, H. F. Monolithic Dual-Wedge Prism-Based Spectroscopic Single-Molecule Localization Microscopy. *Nanophotonics* **2022**, *11*, 1527–1535.
(25) Dong, B.; Soetikno, B. T.; Chen, X.; Backman, V.; Sun, C.; Zhang, H. F. Parallel Three-Dimensional Tracking of Quantum Rods Using Polarization-Sensitive Spectroscopic Photon Localization Microscopy. *ACS Photonics* **2017**, *4*, 1747–1752.
(26) Rimoli, C. V.; Valades-Cruz, C. A.; Curcio, V.; Mavrakis, M.; Brasselet, S. 4polar-STORM Polarized Super-Resolution Imaging of Actin Filament Organization in Cells. *Nat. Commun* **2022**, *13*, 301.
(27) Oleksiievets, N.; Mathew, C.; Thiele, J. C.; Gallea, J. I.; Nevskyi, O.; Gregor, I.; Weber, A.; Tsukanov, R.; Enderlein, J. Single-Molecule Fluorescence Lifetime Imaging Using Wide-Field and Confocal-Laser Scanning Microscopy: A Comparative Analysis. *Nano Lett.* **2022**, *22*, 6454–6461.
(28) Thiele, J. C.; Helmerich, D. A.; Oleksiievets, N.; Tsukanov, R.; Butkevich, E.; Sauer, M.; Nevskyi, O.; Enderlein, J. Confocal Fluorescence-Lifetime Single-Molecule Localization Microscopy. *ACS Nano* **2020**, *14*, 14190–14200.
(29) Xiang, L.; Chen, K.; Xu, K. Single Molecules Are Your Quanta: A Bottom-Up Approach toward Multidimensional Super-Resolution Microscopy. *ACS Nano* **2021**, *15*, 12483–12496.
(30) Honglin Li; Joshua C. Vaughan. Switchable Fluorophores for Single-Molecule Localization Microscopy. *Chem. Rev.* **2018**, *118,* 9412–9454
(31) Aparin, I. O.; Yan, R.; Pelletier, R.; Choi, A. A.; Danylchuk, D. I.; Xu, K.; Klymchenko, A. S. Fluorogenic Dimers as Bright Switchable Probes for Enhanced Super-Resolution Imaging of Cell Membranes. *J. Am. Chem. Soc.* **2022**, *144*, 18043–18053.
(32) Chozinski, T. J.; Gagnon, L. A.; Vaughan, J. C. Twinkle, Twinkle Little Star: Photoswitchable Fluorophores for Super-Resolution Imaging. *FEBS Lett.* **2014**, *588*, 3603–3612.
(33) Minoshima, M.; Kikuchi, K. Photostable and Photoswitching Fluorescent Dyes for Super-Resolution Imaging. *J. Biol. Inorg. Chem.* **2017**, *22*, 639–652.
(34) van de Linde, S.; Sauer, M. How to Switch a Fluorophore: From Undesired Blinking to Controlled Photoswitching. *Chem. Soc. Rev.* **2014**, *43*, 1076–1087.
(35) Grimm, J. B.; English, B. P.; Choi, H.; Muthusamy, A. K.; Mehl, B. P.; Dong, P.; Brown, T. A.; Lippincott-Schwartz, J.; Liu, Z.; Lionnet, T.; Lavis, L. D. Bright Photoactivatable Fluorophores for Single-Molecule Imaging. *Nat. Methods* **2016**, *13*, 985–988.
(36) Brenner, B.; Sun, C.; Raymo, F. M.; Zhang, H. F. Spectroscopic Single-Molecule Localization Microscopy: Applications and Prospective. *Nano Converg.* **2023**, *10*, 14.
(37) Bates, M.; Huang, B.; Dempsey, G. T.; Zhuang, X. Multicolor Super-Resolution Imaging with Photo-Switchable Fluorescent Probes. *Science* **2007**, *317*, 1749–1753.
(38) Zhang, Y.; Wang, G.; Huang, P.; Sun, E.; Kweon, J.; Li, Q.; Zhe, J.; Ying, L. L.; Zhang, H. F. Minimizing Molecular Misidentification in Imaging Low-Abundance Protein Interactions Using Spectroscopic Single-Molecule Localization Microscopy. *Anal. Chem.* **2022**, *94*, 13834–13841.
(39) Zhang, Y.; Zhang, Y.; Song, K. H.; Lin, W.; Sun, C.; Schatz, G. C.; Zhang, H. F. Investigating Single-Molecule Fluorescence Spectral Heterogeneity of Rhodamines Using High-Throughput Single-Molecule Spectroscopy. *J. Phys. Chem. Lett.* **2021**, *12*, 3914–3921
(40) Zhang, Y.; Schroeder, L. K.; Lessard, M. D.; Kidd, P.; Chung, J.; Song, Y.; Benedetti, L.; Li, Y.; Ries, J.; Grimm, J. B.; Lavis, L. D.; De Camilli, P.; Rothman, J. E.; Baddeley, D.; Bewersdorf, J. Nanoscale Subcellular Architecture Revealed by Multicolor Three-Dimensional Salvaged Fluorescence Imaging. *Nat. Methods* **2020**, *17*, 225–231.
(41) Song, K.-H.; Zhang, Y.; Wang, G.; Sun, C.; Zhang, H. F. Three-Dimensional Biplane Spectroscopic Single-Molecule Localization Microscopy. *Optica* **2019**, *6*, 709–715.
(42) Song, K.-H.; Dong, B.; Sun, C.; Zhang, H. F. Theoretical Analysis of Spectral Precision in Spectroscopic Single-Molecule Localization Microscopy. *Rev. Sci. Instrum.* **2018**, *89*, 123703.
(43) Abdelsayed, V.; Boukhatem, H.; Olivier, N. An Optimized Buffer for Repeatable Multicolor STORM. *ACS Photonics* **2022**, *9*, 3926–3934.
(44) Sharonov A, Hochstrasser RM. Wide-field subdiffraction imaging by accumulated binding of diffusing probes. *Proc. Natl. Acad. Sci. U.S.A.* **2006**, *103*,18911-18916.
(45) Yan, R.; Moon, S.; Kenny, S. J.; Xu, K. Spectrally Resolved and Functional Super-Resolution Microscopy via Ultrahigh-Throughput Single-Molecule Spectroscopy. *Acc. Chem. Res.* **2018**, *51*, 697–705.
(46) Backlund, M. P.; Lew, M. D.; Backer, A. S.; Sahl, S. J.; Moerner, W. E. The Role of Molecular Dipole Orientation in Single-Molecule Fluorescence Microscopy and Implications for Super-Resolution Imaging. *ChemPhysChem* **2014**, *15*, 587–599.
(47) Reuss, M.; Engelhardt, J.; Hell, S. W. Birefringent Device Converts a Standard Scanning Microscope into a

STED Microscope That Also Maps Molecular Orientation. *Opt. Express* **2010**, *18*, 1049–1058.
(48) Xiang, L.; Yan, R.; Chen, K.; Li, W.; Xu, K. Single-Molecule Displacement Mapping Unveils Sign-Asymmetric Protein Charge Effects on Intraorganellar Diffusion. *Nano Lett.* **2023**, *23*, 1711–1716.
(49) Choi, A. A.; Xiang, L.; Li, W.; Xu, K. Single-Molecule Displacement Mapping Indicates Unhindered Intracellular Diffusion of Small (≲1 KDa) Solutes. *J. Am. Chem. Soc.* **2023**, *145*, 8510–8516.
(50) Sansalone, L.; Zhang, Y.; Mazza, M. M. A.; Davis, J.; Song, K. H.; Captain, B.; Zhang, H. F.; Raymo, F. M. High-Throughput Single-Molecule Spectroscopy Resolves the Conformational Isomers of BODIPY Chromophores. *J. Phys. Chem. Lett.* **2019**, *10*, 6807–6812
(51) Kim, D.; Zhang, Z.; Xu, K. Spectrally Resolved Super-Resolution Microscopy Unveils Multipath Reaction Pathways of Single Spiropyran Molecules. *J. Am. Chem. Soc.* **2017**, *139*, 9447–9450.
(52) Lu, H. P.; Xie, X. S. Single-Molecule Spectral Fluctuations at Room Temperature. *Nature* **1997**, *385*, 143–146.
(53) Boens, N.; Leen, V.; Dehaen, W. Fluorescent Indicators Based on BODIPY. *Chem. Soc. Rev.* **2012**, *41*, 1130–1172.
(54) Cao, D.; Liu, Z.; Verwilst, P.; Koo, S.; Jangjili, P.; Kim, J. S.; Lin, W. Coumarin-Based Small-Molecule Fluorescent Chemosensors. *Chem. Rev.* **2019**, *119*, 10403–10519.
(55) Han, J.; Burgess, K. Fluorescent Indicators for Intracellular PH. *Chem. Rev.* **2010**, *110*, 2709–2728.
(56) Nahidiazar, L.; Agronskaia, A. V.; Broertjes, J.; Broek, B. van den; Jalink, K. Optimizing Imaging Conditions for Demanding Multi-Color Super Resolution Localization Microscopy. *PLOS ONE* **2016**, *11*, e0158884.
(57) Schlichthaerle, T.; Strauss, M. T.; Schueder, F.; Auer, A.; Nijmeijer, B.; Kueblbeck, M.; Jimenez Sabinina, V.; Thevathasan, J. V.; Ries, J.; Ellenberg, J.; Jungmann, R. Direct Visualization of Single Nuclear Pore Complex Proteins Using Genetically-Encoded Probes for DNA-PAINT. *Angew. Chem. Int. Ed. Engl.* **2019**, *58*, 13004–13008.
(58) Jungmann, R.; Avendaño, M. S.; Dai, M.; Woehrstein, J. B.; Agasti, S. S.; Feiger, Z.; Rodal, A.; Yin, P. Quantitative Super-Resolution Imaging with QPAINT. *Nat. Methods* **2016**, *13*, 439.
(59) Zhang, Y.; Raymo, F. M. Live-Cell Imaging at the Nanoscale with Bioconjugatable and Photoactivatable Fluorophores. *Bioconjugate Chem.* **2020**, *31*, 1052–1062
(60) Fölling, J.; Bossi, M.; Bock, H.; Medda, R.; Wurm, C. A.; Hein, B.; Jakobs, S.; Eggeling, C.; Hell, S. W. Fluorescence Nanoscopy by Ground-State Depletion and Single-Molecule Return. *Nat. Methods* **2008**, *5*, 943–945.
(61) Zheng, Q.; Juette, M. F.; Jockusch, S.; Wasserman, M. R.; Zhou, Z.; Altman, R. B.; Blanchard, S. C. Ultra-Stable Organic Fluorophores for Single-Molecule Research. *Chem. Soc. Rev.* **2014**, *43*, 1044–1056.
(62) Altman, R. B.; Terry, D. S.; Zhou, Z.; Zheng, Q.; Geggier, P.; Kolster, R. A.; Zhao, Y.; Javitch, J. A.; Warren, J. D.; Blanchard, S. C. Cyanine Fluorophore Derivatives with Enhanced Photostability. *Nat. Methods* **2011**, *9*, 68–71.
(63) Grimm, J. B.; Muthusamy, A. K.; Liang, Y.; Brown, T. A.; Lemon, W. C.; Patel, R.; Lu, R.; Macklin, J. J.; Keller, P. J.; Ji, N.; Lavis, L. D. A General Method to Fine-Tune Fluorophores for Live-Cell and in Vivo Imaging. *Nat. Methods* **2017**, *14*, 987–994.
(64) Chen, J.; Yao, B.; Yang, Z.; Shi, W.; Luo, T.; Xi, P.; Jin, D.; Li, Y. Ratiometric 4Pi Single-Molecule Localization with Optimal Resolution and Color Assignment. *Opt. Lett.* **2022**, *47*, 325–328.
(65) Gu, L.; Li, Y.; Zhang, S.; Xue, Y.; Li, W.; Li, D.; Xu, T.; Ji, W. Molecular Resolution Imaging by Repetitive Optical Selective Exposure. *Nat. Methods* **2019**, *16*, 1114–1118.
(66) Reymond, L.; Ziegler, J.; Knapp, C.; Wang, F.-C.; Huser, T.; Ruprecht, V.; Wieser, S. SIMPLE: Structured Illumination Based Point Localization Estimator with Enhanced Precision. *Opt. Express* **2019**, *27*, 24578–24590.
(67) Nehme, E.; Weiss, L. E.; Michaeli, T.; Shechtman, Y. Deep-STORM: Super-Resolution Single-Molecule Microscopy by Deep Learning. *Optica* **2018**, *5*, 548-464
(68) Speiser, A.; Müller, L.-R.; Hoess, P.; Matti, U.; Obara, C. J.; Legant, W. R.; Kreshuk, A.; Macke, J. H.; Ries, J.; Turaga, S. C. Deep Learning Enables Fast and Dense Single-Molecule Localization with High Accuracy. *Nat. Methods* **2021**, *18*, 1082–1090.
(69) Kim, T.; Moon, S.; Xu, K. Information-Rich Localization Microscopy through Machine Learning. *Nat. Commun* **2019**, *10*, 1996.
(70) Möckl, L.; Roy, A. R.; Petrov, P. N.; Moerner, W. E. Accurate and Rapid Background Estimation in Single-Molecule Localization Microscopy Using the Deep Neural Network BGnet. *Proc. Natl. Acad. Sci. U.S.A.* **2020**, *117*, 60–67.
(71) Kumar Gaire, S.; Zhang, Y.; Li, H.; Yu, R.; Zhang, H. F.; Ying, L. Accelerating Multicolor Spectroscopic Single-Molecule Localization Microscopy Using Deep Learning. *Biomed. Opt. Express* **2020**, *11*, 2705–2721.
(72) Du, W.; Tian, H. Transformer and GAN Based Super-Resolution Reconstruction Network for Medical Images. arXiv:**2022**, 2212.13068.
(73) Qiao, C.; Li, D.; Liu, Y.; Zhang, S.; Liu, K.; Liu, C.; Guo, Y.; Jiang, T.; Fang, C.; Li, N.; Zeng, Y.; He, K.; Zhu, X.; Lippincott-Schwartz, J.; Dai, Q.; Li, D. Rationalized Deep Learning Super-Resolution Microscopy for Sustained Live Imaging of Rapid Subcellular Processes. *Nat. Biotechnol.* **2023**, *41*, 367–377.

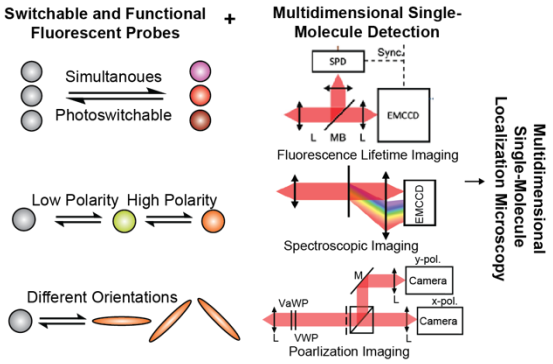
Switchable and Functional Fluorescent Probes
+
Multidimensional Single-Molecule Detection
Simultanoues
Photoswitchable
Low Polarity
High Polarity
Different Orientations
SPD
Sync
EMCCD
L
MB
L
Fluorescence Lifetime Imaging
EMCCD
Spectroscopic Imaging
M
y-pol.
Camera
L
VaWP
x-pol.
Camera
L
VWP
L
Poarlization Imaging
Multidimensional Single-Molecule Localization Microscopy